Chapter 9

High-Speed Single-Photon Detection with Avalanche Photodiodes in the Near Infrared

Yan Liang and Heping Zeng

Additional information is available at the end of the chapter

http://dx.doi.org/10.5772/60481

Abstract

As the requisite optical components in quantum information processing, single-photon detectors of high performance at the near-infrared wavelengths are in urgent need. In this paper, we review our recent development in high-speed single-photon detection with avalanche photodiodes, increasing the working repetition frequency up to GHz. Ingenious techniques, such as capacitance-balancing, self-differencing, low-pass filtering, and frequency up-conversion, were employed to achieve high-speed single-photon detection with high detection efficiency and low error counts, offering facility for many important applications, such as laser ranging and imaging, quantum key distribution at GHz clock rate.

Keywords: Avalanche photodiode, Single-photon detection, Single-photon frequency up-conversion, Quantum key distribution

1. Introduction

Single-photon detectors (SPDs), which are sufficiently sensitive to register single-photon clicks, are widely used in numerous fields of great importance, such as positron emission tomography, optical time domain reflectometry, astronomy and deep-space communication, and biological imaging [1-6]. SPDs are extraordinarily essential not only in fundamental research of quantum physics [7, 8], but also in practical quantum information processing techniques [9-11]. As one of the most commercially successful quantum information applications, quantum key distribution (QKD), which makes it possible for two distant parties to share secret keys via telecommunication, has rapidly progressed since its initial proposal in 1984 [12–16]. In order to achieve efficient QKD of long distances, GHz-clocked QKD systems have been developed. In these schemes, high-speed SPDs of high detection efficiency and low noise at

the telecommunication wavelengths are necessary to guarantee the performance of high-speed QKDs [17-18]. Moreover, as for another revolutionary quantum information application, linear optical quantum computing (LOQC), which is a scalable paradigm for quantum information processing and computation, remains difficult to achieve [19-20]. Many efforts have been made worldwide toward this goal. A major factor that limits the advance of LOQC is the performances of the optical components such as SPDs. Significant improvements are still needed in terms of their detection efficiency, error counts, and ability to resolve photon numbers.

Thus far, many concepts and techniques have been proposed to realize high-performance single-photon detection. For instance, single-photon avalanche photodiodes (SPADs), SPDs based on frequency up-conversion, visible-light photon counters, superconducting transition-edge sensors, superconducting nanowire SPDs (SNSPDs), and SPDs based on quantum dots and semiconductor defects, differ in terms of spectral response, quantum efficiency, dark count and afterpulse noise, signal-to-noise ratio, timing jitter, and photon-number-resolving capability, providing optimal choices for various specific applications [21-28]. In consideration of high-speed quantum information processing applications, SPADs, frequency up-conversion technique, and SNSPDs are competitive choices [29-31]. Although SNSPDs possess the characteristic of ultra-low noise and timing jitter, which enables hundreds-of-kilometers QKD system, the requirement of cryogenic cooling system is one of the obvious drawbacks for practical applications. In this chapter, we focus on the recent development of high-speed single-photon detection based on InGaAs/InP SPADs and frequency up-conversion in the near infrared. Since the basic principle of the frequency up-conversion is to translate a near-infrared photon to the visible regime and then detect the photon with silicon avalanche photodiodes, the content presented in the following sections is concluded to be high-speed single-photon detection with avalanche photodiodes in the near infrared.

For their compact structure and low-power consumption, InGaAs/InP SPADs have been used intensively in practical applications at the near-infrared wavelengths, especially in QKD and laser ranging and imaging systems [32-34]. The avalanche photodiode (APD) is reverse-biased above the breakdown voltage (which is called Geiger operation mode), and carriers generated by a single-photon absorption could trigger a detectable macroscopic current after the avalanche gain. To make use of this avalanche propagation progress adequately, the avalanche should be stopped and the APD reset with a peripheral circuit. Generally, InGaAs/InP SPADs are operated in gated Geiger mode that employs gating pulse to determine the switching of the APD's bias voltage between overvoltage and undervoltage. In this operation mode, the dark counts of InGaAs/InP SPADs would be reduced effectively [35-37]. However, since the APD is a capacitive device, the spike noise produced by the gating pulses charging and discharging on the APD's capacitance is an inevitable problem. The weak photon-induced avalanche signals are buried in the spike noise, making the key technique to improve the performance of InGaAs/InP SPADs lie in efficient discrimination of avalanche signals from the spike noise. Furthermore, with the increase of the working repetition frequency, the afterpulsing effect becomes more and more serious, greatly affecting the performance of InGaAs/InP SPADs. The afterpulses are the error counts induced by the release of carriers trapped by defects in the multiplication region during an earlier avalanche event. To solve this

http://dx.doi.org/10.5772/60481

issue, the avalanche gain should be decreased correspondingly, unavoidably resulting in the increase of the difficulty in the extraction of the valid avalanche signals.

Recently, some artful techniques, such as sinusoidal gating, self-differencing, and the combination of both, have been demonstrated to suppress the spike noise efficiently while increase the gating repetition rate over 1 GHz [38-42]. In a sinusoidal gating circuit, the spike noise produced by the applied sinusoidal gates was well cancelled by the specific electric band-elimination filters, considering that the APD's capacitive response exhibits a relatively simple frequency spectrum. The InGaAs/InP SPADs that made use of this technique could be operated at 1.5 GHz with the detection efficiency of 10.8% [38]. Comparatively, the spike noise in the self-differencing scheme was eliminated by comparing the output of the APD with that delayed by one gating cycle. This type of SPAD was able to work at 1.25 GHz with the detection efficiency of 10.9% and dark count rate of 2.34×10^{-6} per gate [40]. Besides, the technique of harmonic subtraction was put forward to achieve high detection efficiency and low afterpulse probability for high-speed single-photon detection [43]. With this method, the detection efficiency of InGaAs/InP SPADs could reach ~ 50% with afterpulse probability below 3.5×10^{-4} per gate at 1.25 GHz. Although, all these approaches performed admirably, they are far from mature. There is still room for further enhancement in the respects of dark counts, maximum count rate, and timing jitter.

On the other hand, given the mature silicon SPD with high performance, the frequency up-conversion single-photon detection has shown great potential for many applications. Its basic principle is to translate a near-infrared photon to the visible regime, avoiding the disadvantages of InGaAs/InP APDs [44-46]. This nonlinear optics process requires a large nonlinearity of the nonlinear media and a strong pump field to realize the complete quantum conversion. Generally, the strong pump could be achieved by an external cavity or intracavity enhancement or a waveguide confinement, inevitably bringing about severe background noise because of the parasitic nonlinear interactions. Synchronized single-photon frequency up-conversion was presented to lower the noise. For the improvement of the conversion efficiency, the specific control of the synchronized pulses was required. Recently, efficient single-photon frequency up-conversion detection system operating at tens of MHz has been realized based on the all-optical synchronized fiber lasers, promising its applications in high-speed QKDs.

In this chapter, our recent developments and achievements in high-speed single-photon detection based on InGaAs/InP SPAD and frequency up-conversion single-photon detection were introduced in detail. In Section II, we present the experimental demonstration on some innovative schemes for InGaAs/InP SPAD, such as the optically self-differencing, the low-pass filtering with ultrashort pulses, and the creative combination of the self-differencing and low-pass filtering, to increase the working repetition frequency of the gated SPAD over 1 GHz. Meanwhile, other properties of the SPAD, for instance, the detection efficiency, the timing jitter, and the maximum counts, have been improved as well. Furthermore, a compact synchronized fiber laser system for highly efficient single-photon frequency up-conversion is illustrated in Section III, realizing high conversion efficiency with low background counts. All these high-performance single-photon detectors provide essential facility for high-speed quantum information applications. In Section IV, we discuss the advantage of the high-speed

single-photon detection in some applications, such as laser ranging and imaging, quantum key distribution, and so on. Finally, we conclude the chapter in the last section by emphasizing the importance of the high-speed single-photon detection for quantum information applications.

2. Single-photon avalanche photodiodes

As mentioned in the introduction, the suppression ratio of the spike noise, which is generated by the capacitive response of the APD to the gating pulses, is quite critical to the performance of InGaAs/InP SPAD operated in gated Geiger mode. In this section, we present several methods to remove spike noise and acquire avalanche signals, achieving high-speed SPAD with excellent properties.

2.1. Capacitance balancing technique

Since the spike noise is caused by the capacitance characteristics of the APD, the capacitance-balancing technique employs a capacitor to imitate the APD's response. As shown in Fig. 1 (a), the InGaAs/InP APD was connected in parallel with a complementary capacitor. The output signals of the APD and capacitor were connected to the 0 and π inputs of the magic-T network (MTNT), respectively. The MTNT was used as a subtracter here, subtracting the two spike noises from the APD and the capacitor. A tunable capacitor was chosen for the perfect matching between the APD and the complementary capacitor. Then, at the output of the circuit, only the avalanche signal was extracted and acquired by an oscilloscope after amplification by an RF amplifier.

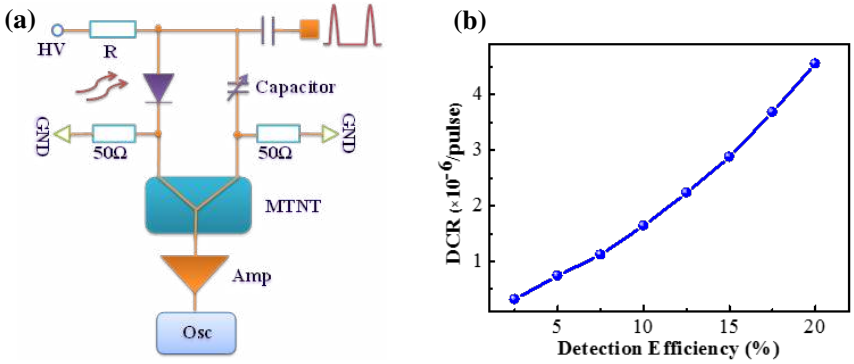

Figure 1. (a) Schematic setup of capacitance-balancing InGaAs/InP SPAD. MTNT: a so-called magic-T network consisted with a broadband transformer; Amp: an RF amplifier; Osc: a high bandwidth oscilloscope. (b) Dark count rate of capacitance-balancing InGaAs/InP SPAD as a function of detection efficiency at 100 MHz.

In the capacitance-balancing scheme, the repetition frequency of the gating pulses could be tuned continuously on a large scale. Moreover, the capacitance-balancing InGaAs/InP SPADs

are suitable for the applications requiring multi-channel timing acquisition, such as the time-code quantum key distribution. We just need to adjust the tunable capacitor to ensure the suppression ratios of the spike noise. A train of double gating pulses was employed to illustrate the capability of multi-channel detection. By changing the time interval between the double gating pulses, we could obtain that the capacitance balancing technique remained applicable in the single-photon detection with the gating repetition rate no higher than 260 MHz [47].

Here, we examined the performance of the SPADs at 100 MHz. The amplitude of the gating pulses was 4 V with the duration of ~ 1 ns, while the DC bias applied on the APD was varied to obtain different detection efficiencies. The operation temperature of the InGaAs/InP APD was set at -50℃. And a 1550-nm pulsed laser at 10 MHz with full width at half maximum (FWHM) of ~35 ps was attenuated to contain 0.1 photon per pulse before coupling into the APD fiber pigtail as the photon source. The laser pulse was synchronously triggered with the gating pulse, while their delay was adjusted to gain the highest detection efficiency for optimized operation. Figure 1 (b) exhibited the dark count rates as a function of the detection efficiency. The dark count rate increased with the detection efficiency, and we could figure out that the dark count rate was approximately 4.6×10^{-6} with the efficiency of 20%, indicating this SPAD performed well at 100 MHz.

Unlike the double-APD balancing [48], the capacitance-balancing technology using a capacitor instead to imitate the APD was much more economic and practical. The suppression ratio of the spike noise was ~ 19 dB, limiting the working speed. We believe that the capacitance-balancing SPAD would be able to be operated at a higher speed with the advance of semiconductor techniques.

2.2. Self-differencing technique

The self-differencing technique first proposed by Z. L. Yuan et al. has shown a great improvement of the detection speed. Recently, the InGaAs/InP SPAD using this method has been shown to perform remarkably with the detection efficiency of 25% and dark count rate of 5.9×10^{-5} per gate at 1 GHz without Peltier cooling [49]. Unlike the traditional self-differencing circuits, we added a tunable phase shifter and attenuator for better suppression of the spike noise, as demonstrated in Fig. 2 (a). The gating pulses were superposed on the reversely biased InGaAs/InP APD. The output signal of the APD was sent to a 50/50 power splitter (DC to 3 GHz), being divided into two identical components. Then one component was delayed by one gating period through the tunable phase shifter, and the tunable attenuator in the other arm was used to guarantee equal amplitudes.

Afterward the two components were combined by a differencer (DC to 3 GHz) before amplification. The output of the circuit was the amplified difference between the two split components, shifted relatively by one gating period. The tunable phase shifter and attenuator precisely controlled the split two components, ensuring the avalanche signal extracted with spike noise suppressed greatly. Furthermore, with the tunable phase shifter, the working repetition frequency of the self-differencing SPAD could be adjusted continuously with ease. And the adjustment range was determined by that of the phase shifter.

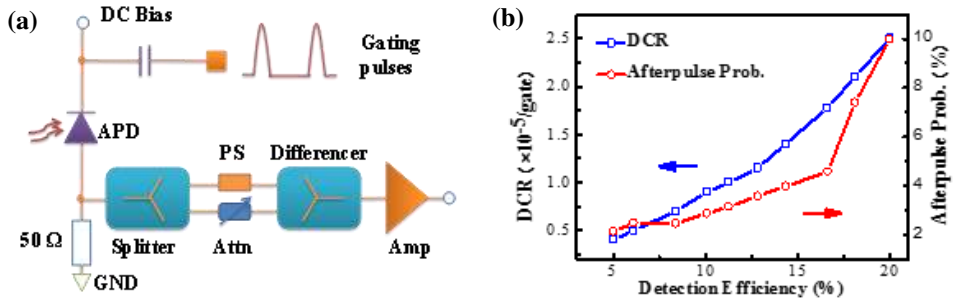

Figure 2. (a) Experimental setup of the self-differencing InGaAs/InP SPAD. PS: tunable phase shifter, Attn: tunable attenuator, Amp: RF amplifier. (b) Dark count rate and afterpulse probability as a function of the detection efficiency at –40℃.

The 200-MHz gating pulses with amplitude of 5 V and duration of ~ 1 ns were used to characterize the performance of this InGaAs/InP SPAD. And the InGaAs/InP APD was cooled to be -40℃. Figure 2 (b) displayed the dark count rate and afterpulse probability as a function of detection efficiency. The reverse bias voltage applied on the APD was changed to obtain different efficiencies. The laser source was attenuated to contain 0.1 photons per pulse on average. The detection efficiency was corrected for Poissonian statistics of the photon numbers by the formula

$$1 - e^{-\mu \cdot \eta} = R_O \left(1 - P_E\right) / R_L \langle \mu \rangle \tag{1}$$

where η was the detection efficiency, R_O was the overall counting rate, R_L was the repetition rate of the laser pulse, P_E was the error counting probability, and μ was the average photon per pulse. In the experimental measurement, the dark count rate was measured with the laser off. It increased gradually with the detection efficiency.

The afterpulse probability, defined as the ratio of the total afterpulse counts to the photon counts, can be calculated from

$$P_A = \frac{\left(I_{NI} - I_D\right)}{I_{ph} - I_{NI}} R \tag{2}$$

where I_{Ph} and I_{NI} were the count rate per gate at the illuminated and nonilluminated gates, respectively, while I_D was the dark count rate for each gate. R was the ratio of the repetition frequency of the gating pulse to that of the laser pulse. Here we took R=20 for measuring the afterpulse. The afterpulse probability increased with the detection efficiency and began to increase dramatically when the detection efficiency reached 16.7%, greatly impacting the performance of the SPAD. When the detection efficiency was 10.1%, the afterpulse probability was just 2.9% and the corresponding dark count rate was 9.0×10^{-6} per gate.

http://dx.doi.org/10.5772/60481

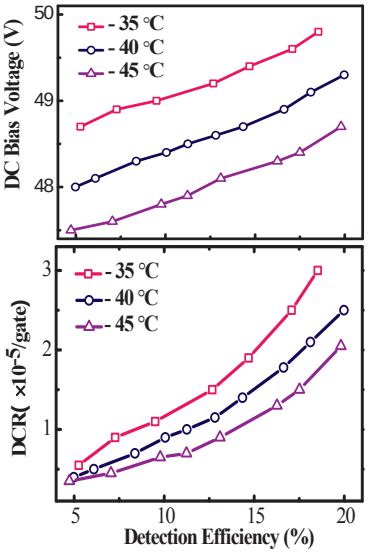

Figure 3. DC bias voltage applied on APD and dark count rate as a function of detection efficiency at three different temperatures.

The operation temperature of the InGaAs/InP APD was vital to the SPAD. We Peltier-cooled the APD to work at three different temperatures and tested the parameters of the SPAD. Figure 3 showed the dc voltage and dark count rate as a function of the dc bias voltage. The detection efficiency increased with the voltage. Meanwhile the rising slopes were almost the same at the three temperatures. To achieve the same detection efficiency, we should apply higher voltage at higher temperature. Since the gating pulses were identical, it could be figured out that the breakdown voltage increased with the temperature of the APD, leading to a great influence on the SPAD. Meanwhile, the dark count rate increased with the detection efficiency, while it was higher at the same efficiency at higher temperature. However, cooling the APD to lower temperatures consumes more energy. Therefore, we should choose an appropriate temperature in practical applications.

Furthermore, the InGaAs/InP SPAD using the cascade of self-differencing circuits was demonstrated [50]. By introducing a second self-differencing circuit, the suppression ratio was enhanced up to ~18 dB, making the SPAD more suitable for high-speed applications. Considering the twice splitting of the valid avalanche signal, the signal-to-noise ratio (SNR) was merely improved by ~10 dB.

We also proposed the optically self-balancing technique, as exhibited in Fig. 4 [51-53]. The output of the InGaAs/InP APD was amplified to trigger a laser diode at 1550 nm. Then, an erbium-doped fiber amplifier (EDFA) was used to magnify the transformed optical signal. Afterward, the splitting and the relative delay of the signal were processed through the optical devices. Finally, the avalanche signal was extracted and transformed to the electronic signal

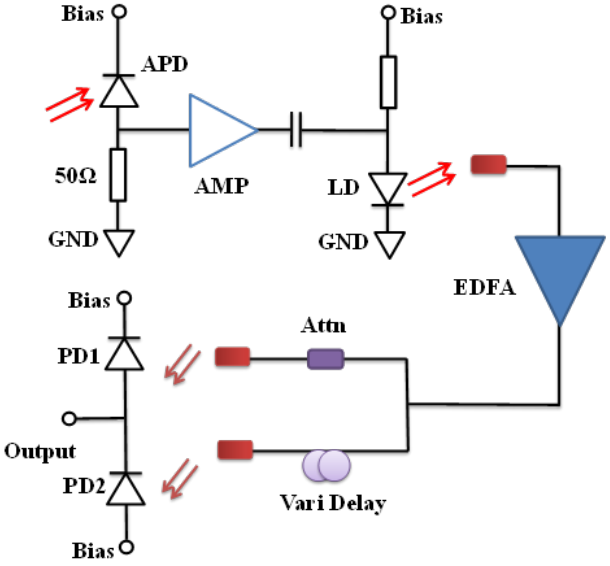

Figure 4. Schematic setup of the optically self-balancing SPAD. AMP: RF amplifier; LD: distributed-feedback laser diode at 1550 nm; Attn: tunable optical attenuator; and PD1; 2: pin photodiodes.

by two pin photodiode. Compared to the electronic self-differential technique, the optical method used stable and precisely controllable optical signals, providing immunity to the electromagnetic field of the surrounding circuits. Besides, the impedance matching was not necessary to be considered in this scheme. A 31-dB suppression of the spike noise was obtained, allowing the study on the photon-number resolving dynamics of the InGaAs/InP avalanche photodiode. The detection efficiency reached 22.4% while the afterpulse probability was controlled as low as 2.4% at 25 MHz. However, the transformation between the electronic and optical signal was more and more complicated with the advance of the repetition frequency of the gating pulses superposed on the APD, limiting its applications in high-speed single-photon detection.

The core concepts of the capacitance-balancing and self-differencing techniques are to produce a mimic signal of the spike noise and obtain the valid avalanche signal by making the two signals subtract each other. The performance of the SPAD using those two techniques would be enhanced by improving the similarity of the two signals. In contrast, the technique presented in the next section is to eliminate the spike noise directly by corresponding filters.

2.3. Low-pass filtering technique

N. Namekata et al. first put forward the sinusoidal gating technique, employing the sinusoidal gates to control the bias voltage of the InGaAs/InP APD. The frequency distribution of the capacitive response of the APD to the sinusoidal gates was relatively simple, mainly concentrating at the repetition frequency of the gates and its harmonic frequencies. Notch filters were

http://dx.doi.org/10.5772/60481

used to eliminate the spike noise and obtain the avalanche signal. The scheme suppressed the spike noise robustly and conveniently. By this means, the detection efficiency of the SPAD reached 10.5% with a dark count rate of 6.1×10^{-7} per gate and afterpulse probability of 3.4% at 2 GHz [39]. However, due to the distortion of the avalanche signal caused by the notch filters, the timing jitter of this SPAD was as large as 180 ps, limiting its applications in high-speed QKD systems or ultra-sensitive long-distance laser ranging. To solve this problem, we proposed the low-pass filtering technology, maintaining the suppression ratio of the spike noise while reducing the timing jitter.

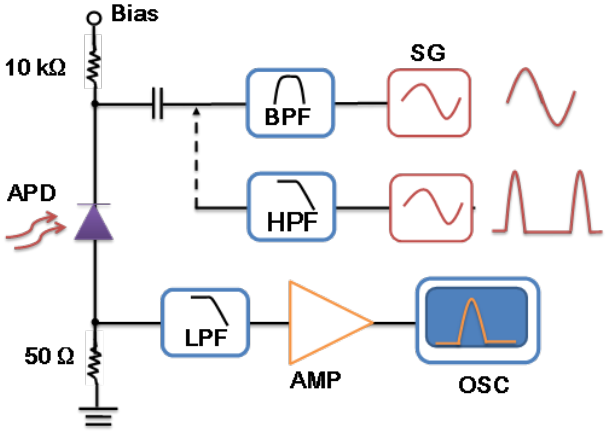

Figure 5. Schematic setup of the low-pass filtering SPAD using sinusoidal gates and ultrashort gating pulses. SG: signal generator; BPF: band-pass filter; HPF: high-pass filter; LPF: low-pass filter.

Figure 5 illustrated the low-pass filtering technology. Before being applied on the APD, the sinusoidal gates passed through a band-pass filter to eliminate the sideband noise and harmonic noise. We used 1.5-GHz sinusoidal waves to examine the performance of the low-pass filtering InGaAs/InP SPAD. The output of the APD was filtered by the low-pass filtering cutting off at 1 GHz with the attenuation higher than 40 dB at 1.5 GHz. Since the spectrum of the avalanche signal distributed mostly at low frequency under 1 GHz, while that of the spike noise concentrated at 1.5 GHz and its harmonic frequencies, we could acquire the avalanche signal by the low-pass filter. To obtain higher SNR, we could employ one more low-pass filter.

The operation temperature of the APD was set at -30℃. The laser source was attenuated to contain one photon per pulse on average to shorten the time of data acquisition, and synchronously triggered with the sine wave frequency. The amplitude of the amplified sinusoidal gating waves was fixed at 6 V. Figure 6 (a) illustrated the performance of the SPAD. The dark count rate and afterpulse probability increased with the detection efficiency. While the efficiency exceeded ~27%, the afterpulse probability rose sharply, limiting further increase of the detection efficiency. By this approach, the detection efficiency reached 13.0% with a dark-count rate of 1.5×10^{-5} per gate and afterpulse probability of 1.1%. While the detection efficiency

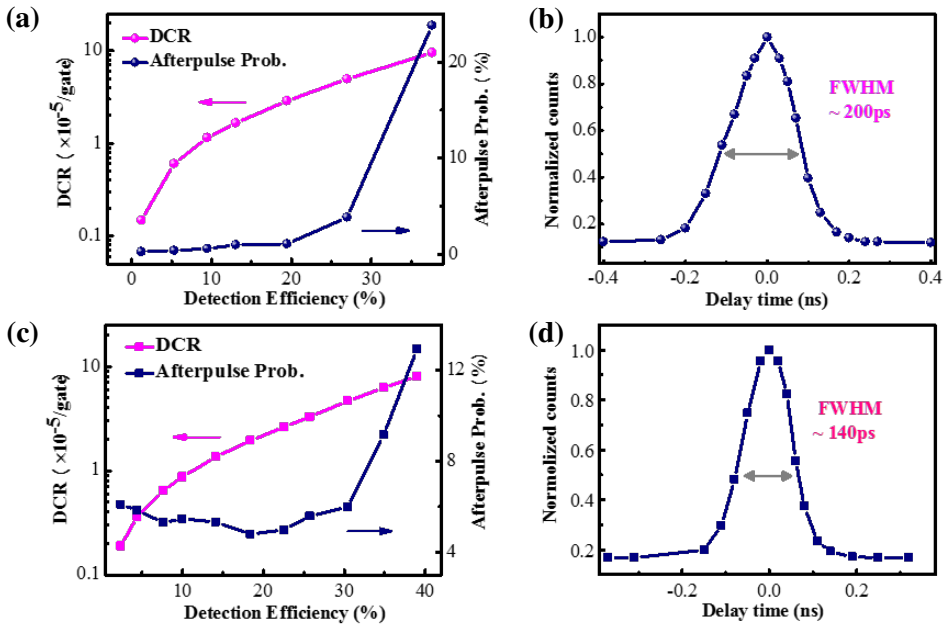

Figure 6. (a) Dark count rate and afterpulse probability of InGaAs/InP SPAD using low-pass filtering technique with sinusoidal gates as a function of the detection efficiency. (b) Count rate dependent on the laser pulse delay in sinusoidally gated SPAD. (c) Dark count rate and afterpulse probability of low-pass filtering SPAD with ultrashort gates as a function of the detection efficiency. (d) Count rate dependent on the laser pulse delay in SPAD with ultrashort gates.

was kept at 10.0%, we adjusted the delay between the laser and sinusoidal gate to get the effective gating width superposed on the APD, as charted in Fig. 6 (b). It was measured to be approximately 200 ps.

Unlike the traditional sinusoidal gating technique, the low-pass filtering was also appropriate for ultrashort gating pulses. We used 1.5-GHz ultrashort gating pulses to characterize the SPAD. The ultrashort pulses were filtered by a high-pass filter (HPF) cutting off at 1 GHz, canceling the noise at low frequencies and ensuring the final SNR of the SPAD. The transmit performance of the HPF remained excellent up to 6 GHz, maintaining the waveform of the ultrashort pulses. The performance of the SPAD was illustrated in Fig. 6 (c). We could find out that the afterpulse probability did not increase obviously until the detection efficiency reached ~ 35%. At the detection efficiency of 35%, the afterpulse probability of the SPAD using ultrashort gating pulses was 9.3% with dark count rate of 6.2×10^{-5} per gate. In comparison, the afterpulse probability of the SPAD using sinusoidal gating pulses was 19.3% with dark count rate of 8.3×10^{-5} per gate. From Fig. 6 (d), it could be noted that the FWHM of the effective gating pulses applied on the APD was 140 ps, less than that in Fig. 6 (b). Since the schematic setup of the two SPADs were exactly the same except the gating signals, we can deduce that ultrashort gating pulses of smaller gating widths improved the SPAD. For a better performance, we could further decrease the gating width.

http://dx.doi.org/10.5772/60481

The timing jitter of the 1.5-GHz SPAD was measured to be 68 ps with a time-correlated single-photon counting (TCSPC) setup (PicoQuant GmbH, PicoHarp 300, Germany). It has been improved a lot by using the low-pass filtering technique, due to the integrity of the avalanche signal preserved well with the low-pass filter. This technology was extraordinarily suitable for high-speed single-photon detection, on account that we could choose low-pass filters cutting off at higher frequencies for better preservation of the avalanche signal. With such a low timing jitter and convenient structure, this type of high-speed SPAD has be widely used in laser ranging systems with high resolution at the near-infrared wavelengths.

2.4. Low-pass filtered self-differencing technique

As mentioned in the previous section, the self-differencing and sinusoidal gating techniques offered effective methods for high-speed single-photon detection. To further advance the suppression ratio of the spike noise, there were schemes to combine the two techniques. However, the SNR was not improved as much, due to the splitting of the avalanche signal in the self-differencing circuit. Here, we introduced some combining techniques to take full advantage of both techniques, achieving high-performance GHz InGaAs/InP SPAD.

Figure 7 (a) exhibited the experimental setup of the SPAD using the combining technique. The sinusoidal wave, which came out from the signal generator, was divided into two parts. One part was amplified to serve as the gating signal superposed on the APD. Here, we set the repetition frequency of the sinusoidal signal to be 1 GHz to characterize the SPAD with this scheme. The output of the APD was filtered by a low-pass filter (LPF1) that cut off at 700 MHz with attenuation higher than 40 dB at 1 GHz. Then it was connected to the power combiner, combined with the other part of the 1-GHz sinusoidal signal. The spectrum of the filtered spike noise concentrated at 1 GHz. The phase shifter was used to make the phase difference between the two signal 180°, and the tunable attenuator was employed to ensure the amplitudes equal. Therefore, we could further eliminate the spike noise and get the avalanche signal, improving the suppression ratio of the spike noise by 21 dB. The low-pass filter (LPF2) cutting off at 1.5 GHz was employed to cancel the electronic noise of high frequency of the cascade RF amplifiers. By this means, the SNR of the SPAD could be advanced with the performance of the timing jitter maintained.

We employed a TCSPC with the resolution of 4 ps to test the timing jitter of the SPAD. As shown in Fig. 7 (b), the time histogram of detection events was recorded. The count peak in the illuminated gating pulse was much higher than the other peaks. The residual peaks after the maximum peak, which might be induced by the oscillation, could be neglected by introducing a proper dead time. Here, a 10-ns dead time was applied. The time interval between the peaks was ~1 ns, matching with the 1-GHz repetition frequency of the sinusoidal gating. And the timing jitter of the avalanche signal showed an FWHM of 60 ps, which was extremely low for sinusoidally gated InGaAs/InP SPAD.

With the 10-ns dead time, we could effectively reduce the error counts. However, it would place a limitation for the maximum counts. We measured the linearity and maximum count rate of the SPAD with a continuous wave laser at 1550 nm to illuminate the APD. As charted in the inset of Fig. 8(b), the photon count rate increased linearly as a function of the photon

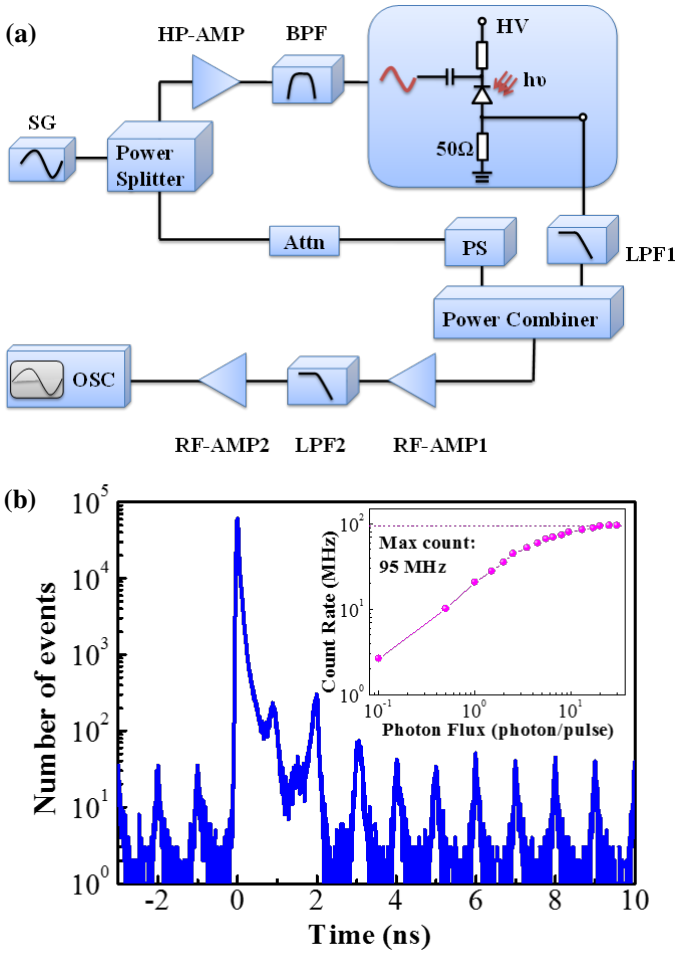

Figure 7. (a) Experimental setup of sinusoidally gated SPAD using low-pass filtered self-differencing technique. SG: signal generator; HP-AMP: high-power amplifier; BPF: band-pass filter; Attn: variable attenuator; LPF1, 2: low-pass filter; RF-AMP1, 2: RF amplifier. (b) Time histogram of detection events recorded by the TCSPC. Inset: Photon detection rate as a function of photon flux.

flux while the counting rate was below 80 MHz. Finally the SPAD was saturated at 95 MHz. The SPAD with such a low timing jitter and high maximum counts provided possibilities for the achievement of high-speed QKD.

As mentioned in the previous section, the performance of the SPAD using the ultrashort gating pulses with shorter duration was even more excellent. We proposed a combining method more appropriate for ultrashort gates, as demonstrated in Fig. 8. In consideration of the distribution of the spike noise, the sinusoidal waves at the repetition rates of f and 2f were added by a power combiner to mimic the spike noise. The differential signal of the output of the APD and

http://dx.doi.org/10.5772/60481

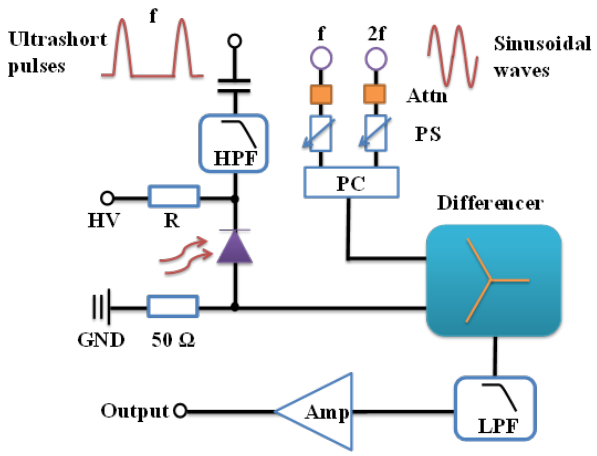

Figure 8. Schematic setup of SPAD using the combining technique with ultrashort gates. HPF: high-pass filter; Attn: tunable attenuator; PS: phase shifter; PC: power combiner; LPF: low-pass filter.

the mimic one was gained and then filtered by a low-pass filter whose cutting-off frequency could be set between 2f and 3f. By this means, the integrity of the avalanche signal could be maintained to the best of the capability of the filtering technique, further reducing the timing jitter of the SPAD. Moreover, the tunable attenuator and phase shifter were used here to guarantee the waveform of the synthetic signal resembles the spike noise as closely as possible. The similarity would advance with the increase of the gating repetition rate, making the scheme quite suitable for high-speed single-photon detection.

The combining technique illustrated earlier took advantages of self-differencing and low-pass filtering technique, achieving high-speed single-photon detection with high suppression ratio and low-timing jitter. With the blossom of the quantum information applications, the SPAD using this technology would be implemented more and more widely.

3. Frequency up-conversion

Frequency conversion plays quite an important role in nonlinear optical signal processing. Infrared single-photon up-conversion based on sum frequency generation was put forward to realize single-photon detection at the infrared wavelengths with existing high-performance Si APDs. Recently, the technique has been successfully used in various applications, including infrared imaging, QKD, and infrared ultra-sensitive spectroscopy [54-56]. More and more interest has been focused on proposing novel schemes for achieving single-photon frequency up-conversion with high efficiency and low noise.

The nonlinear optical media of large nonlinearity and a sufficiently strong pump field were necessary to enforce the complete quantum conversion. Generally, periodically poled lithium

niobate (PPLN) crystal was used as the nonlinear media for nonlinear interaction, considering its relatively large effective nonlinear coefficient and long interaction length. For the requisite strong pump, schemes using an external cavity or intracavity enhancement or a waveguide confinement have been proposed. With such high-intensity pump, frequency up-conversion has been carried out with almost 100% conversion efficiency. However, a strong pump field would unavoidably bring about severe background noise. To solve this problem, synchronized single-photon frequency up-conversion was presented. In the scheme, each signal photon was synchronized to a pump pulse, achieving high efficiencies of frequency up-conversion with quite low noise.

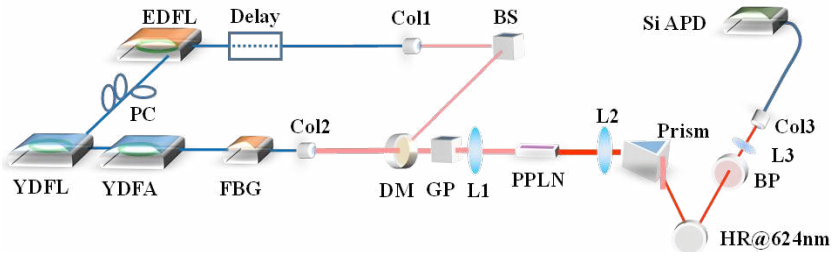

Figure 9. Experimental setup of the synchronous single-photon frequency up-conversion detection. EDFL: erbium-doped fiber laser; YDFL: ytterbium-doped fiber laser; YDFA, ytterbium-doped fiber amplifier; FBG: fiber Bragg grating; Col1, 2, 3: collimator; BS: beam splitter; DM: dichroic mirror; GP: Glan prism; L1, 2, 3: lens; PPLN, periodically poled lithium niobate crystal; BP: optical band-pass filter.

Figure 9 exhibited the experimental setup of the synchronous single-photon frequency up-conversion detection. The signal and pump sources were synchronized in master–slave configuration. The repetition frequency of the synchronized system was about 20.3 MHz. We optimized the spectrum and pulse duration to improve the frequency up-conversion system by managing the intracavity dispersion of the two lasers. The narrow spectrum was required to match with the bandwidth of the PPLN crystal. And the pulse duration of the pump should be a little longer than that of the signal to include all the signal photons within the pump envelop, ensuring the final conversion efficiency.

Figure 10 gave the typical spectra and durations of the signal and pump source. The signal source was provided by an Er-doped NPR locking fiber laser (EDFL), whose output centered at 1562.1 nm with a full width at half maximum (FWHM) of 1.0 nm. The pulse duration was measured to be 1.3 ps by two-photon absorption. The pump source was generated by using an Yb-doped NPR locking fiber laser (YDFL), centering at 1041.1 with an FWHM of 0.7 nm. By self-correlation, the pulse duration was measured to be 34.3 ps. Finally, the 1562.1-nm signal source was up-converted through sum-frequency generation and the up-converted photons at 624 nm were detected by using a standard Si-APD based single-photon detector. The quantum conversion efficiency of infrared photons was up to ~80% with the corresponding background noise of ~300 counts per second. Compared with the background counts of CW pumping, the background was about two orders smaller in synchronously pulsed pumping

http://dx.doi.org/10.5772/60481

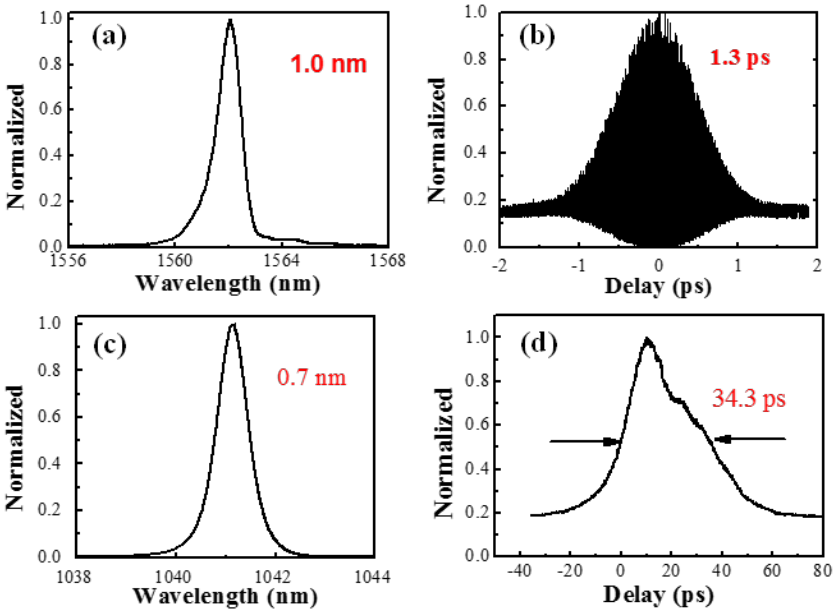

Figure 10. (a) (b) Spectrum and duration of the signal source. The pulse duration was measured by two-photon absorption. (c) (d) Spectrum and duration of the pump source. The pulse duration was measured by self-correlation.

scheme. However, for satisfying the applications of GHz QKD, the single-photon frequency up-conversion technique requires enormous development.

4. Applications in quantum key distribution

Quantum key distribution (QKD) has nowadays been demonstrated as a cryptographic approach to provide absolute security between the sender (Alice) and the receiver (Bob), according to the fundamental laws of quantum mechanics. Fiber-based systems have been implemented in prototype QKD experiments, with practical stabilities in long-distance telecom fibers. The separation distance between Alice and Bob has achieved tens of kilometers in field trials. However, despite these significant advances over recent years QKD's primary challenge is still to obtain higher bit rates over longer distances. The major factors that limit the performance of the QKD are due to the immaturity of single-photon detectors at telecom-wavelengths. The probability of detection decreasing at long distance because of the high losses, while on the other hand, the noise rate of the detector being constant leads to a too high error rate above a certain distance, making it no longer possible to exchange secret keys. Therefore low-noise detectors are essential for long-distance QKD. It could be figured out that with the high-speed SPADs mentioned in the previous section, the performance of QKD systems would be further improved.

Among the fiber-based QKD systems, the polarization-encoding and phase-encoding methods are most widely implemented [57, 58]. Figure 11 showed the schematic setup of polarization-encoding QKD system based on the BB84 four-state protocol. The single-photon signals generated from attenuated laser pulses. Each laser diode could produce only one state of the BB84 protocol. The single-photon signals transmitted through the quantum channel after attenuation and reached Bob's side. As Bob tried to decode the polarization information, he randomly chose HV base or QR base to measure to polarization. Four single-photon detectors (SPD1~ SPD4) were used to detect the single-photon signals. However, in the polarization-encoding QKD system, the polarization states must be aligned and kept aligned due to the imperfection of the optical fiber and the disturbance of the environment. Thus, the polarization real-time control was needed, which presented the main difficulty for the implementation of polarization-encoding QKD system.

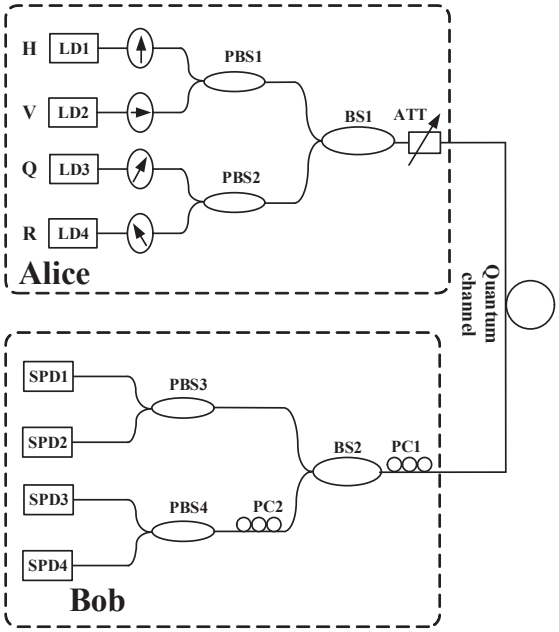

Figure 11. Schematic setup of polarization-coding QKD system. ATT: attenuator, BS: beam splitter, PC: polarization controller, PBS: polarization maintaining beam splitter, SPD: single-photon detector, LD: laser diode.

To examine the applications of the high-speed SPDs in QKD systems, we instead used 1.25-GHz sinusoidally gated InGaAs/InP SPADs to investigate the characteristics of a 1.25 GHz light source at 1550 nm. The laser pulse with the duration of ~20 ps was attenuated to contain 0.01 photon per pulse on average. The dark count rate of the 1.25-GHz SPAD using the low-

pass filtering technique was 8×10^{-6} per gate at the detection efficiency of 10%. The afterpulse probability was ~3.5% with the 10-ns dead time. Figure 12 illustrated the counting rate recorded by the SPAD by changing the delay between the light source and the detector. The extinction ratio of the light pulse was up to 33 dB with the efficient gate width of ~ 140 ps. It could be noted that this SPAD could efficiently achieve high-speed single-photon detection with low error counts, promising its applications in high-speed QKD systems.

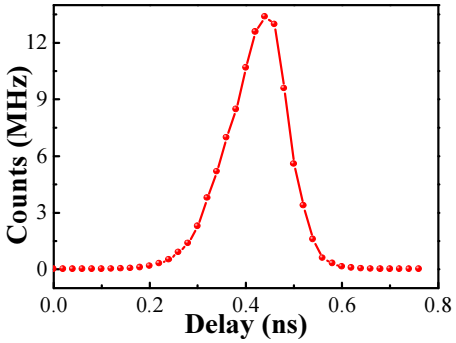

Figure 12. Counting rate depends on the pulse laser delay.

5. Conclusion

In this chapter, we mainly introduced several techniques, such as capacitance-balancing, self-differencing, low-pass filtering, and the combination techniques, to achieve high-speed single-photon detection based on InGaAs/InP SPAD. The spike noise produced by the capacitive response of the APD was well detached, maintaining high efficiency and reducing the error counts correspondingly at GHz working repetition frequency. Furthermore, the frequency up-conversion technique was used to realize infrared single-photon detection with high conversion efficiency and low background noise at ~ 20 MHz. The advance of single-photon detectors highly supported the development of QKD systems, because both the key generation rate and the key distribution distance were mainly limited by the performance of SPDs thus far.

Acknowledgements

This work was supported by the National Natural Science Fund of China (Grant No. 61127014) and the National Key Scientific Instrument Project (Grant No. 2012YQ150092), General Financial Grant from the China Postdoctoral Science Foundation (Grant No. 2014M560347), and the Hujiang Foundation of China (B14002/D14002).

Author details

Yan Liang[1] and Heping Zeng[1,2*]

*Address all correspondence to: yanliangspd@163.com

1 Shanghai Key Laboratory of Modern Optical System, Engineering Research Center of Optical Instrument and System, Ministry of Education, School of Optical-Electrical and Computer Engineering, University of Shanghai for Science and Technology, Shanghai, China

2 State Key Laboratory of Precision Spectroscopy, East China Normal University, Shanghai, China

References

[1] Moehrs S., Guerra A., Herbert D., and Mandelkern M. A detector head design for small-animal PET with silicon photomultipliers (SiPM). Phys. Med. Biol. 2006; 51(5): 1113–1127.

[2] Legre M., Thew R., Zbinden H., and Gisin N. High resolution optical time domain reflectometer based on 1.55um up-conversion photon-counting module. Opt. Exp. 2007; 15(13): 8237–8242.

[3] Degnan J. J. Photon-counting multikilohertz microlaser altimeters for airborne and spaceborne topographic measurements. J. Geodyn. 2002; 34(3–4): 503–549.

[4] Buller G. S., and Wallace A. M. Recent advances in ranging and three-dimensional imaging using time-correlated single-photon counting. IEEE J. Sel. Top. Quantum Electron. 2007; 13: 1006–1015.

[5] Isoshima T., Isojima Y., Hakomori K., Kikuchi K., Nagai K., and Nakagawa H. Ultra-high sensitivity single-photon detector using a Si avalanche photodiode for the measurement of ultraweak biochemiluminescence. Rev. Sci. Instrum. 1995; 66(4): 2922–2926.

[6] Berglund A. J., Doherty A. C., and Mabuchi H. Photon statistics and dynamics of fluorescence resonance energy transfer. Phys. Rev. Lett. 2002; 89: 68101.

[7] Wu E, Rabeau J., Roger G., Treussart F., Zeng H., Grangier P., Prawer S., and Roch J. Room temperature triggered single-photon source in the near infrared. New J. Phys. 2007; 9: 434.

[8] Eisaman M. D., Fan J., Migdall A., and Polyakov S. V. Invited review article: single-photon sources and detectors. Rev. Sci. Instrum. 2011; 82: 71101.

[9] Hadfield R. H. Single-photon detectors for optical quantum information applications. Nat. Photonics 2009; 3: 696–705.

[10] Gabriel C., Wittmann C., Sych D., Dong R., Mauerer W., Andersen U. L., Marquardt C., and Leuchs G. A generator for unique quantum random numbers based on vacuum states. Nat. Photonics 2010; 4: 711–715.

[11] Jian Y., Ren M., Wu E, Wu G. and Zeng H. Two-bit quantum random number generator based on photon-number-resolving detection. Rev. Sci. Instrum. 2011; 82: 073109.

[12] Ekert A. K. Quantum cryptography based on Bell's theorem. Phys Rev Lett 1991; 67: 661–663.

[13] Gisin N., Ribordy G., Tittel W., and Zbinden H. Quantum cryptography. Rev. Mod. Phys. 2002; 74: 145–195.

[14] Hwang W. Quantum key distribution with high loss: toward global secure communication. Phys. Rev. Lett. 2003; 91: 57901.

[15] Wang X. Beating the photon-number-splitting attack in practical quantum cryptography. Phys. Rev. Lett. 2005; 94: 230503.

[16] Takesue H., Harada K., Tamaki K., Fukuda H., Tsuchizawa T., Watanabe T., Yamada K., and Itabashi S. Long-distance entanglement-based quantum key distribution experiment using practical detectors. Opt. Express 2010;18: 6777–6787.

[17] Knill E., Laflamme R., and Milburn G. J. A scheme for efficient quantum computation with linear optics. Nature 2001; 409: 46–52.

[18] Ladd T. D., Jelezko F., Laflamme R., Nakamura Y., Monroe C., and Brien J. L. Quantum computers. Nature 2010; 464: 45–53.

[19] Yuan Z. L., Dixon A. R., Dynes J. F., Sharpe A. W., and Shields A. J. Gigahertz quantum key distribution with InGaAs avalanche photodiodes. Appl. Phys. Lett. 2008; 92(20): 201104.

[20] Rosenberg D., Harrington J. W., Rice P. R., Hiskett P. A., Peterson C. G., Hughes R. J., Lita A. E, Nam S. W., and Nordholt J. E. Long-distance decoy-state quantum key distribution in optical fiber. Phys. Rev. Lett. 2007; 98: 010503.

[21] Cova S., Ghioni M., Lotito A., Rech I., and Zappa F. Evolution and prospects for single-photon avalanche diodes and quenching circuits. J. Mod. Optics 2004; 51: 1267–1288.

[22] Wu G., Zhou C. Y., Chen X. L., and Zeng H. P. High performance of gated-mode single-photon detector at 1.55 μm. Opt. Commun. 2006; 265: 126–131.

[23] Gu X., Huang K., Li Y., Pan H., Wu E., and Zeng H. Temporal and spectral control of single-photon frequency upconversion for pulsed radiation. Appl Phys Lett 2010; 96: 131111.

[24] Waks E., InoueK., Oliver W. D., Diamanti E., and Yamamoto Y. High-efficiency photon-number detection for quantum information processing. IEEE J. Sel. Top. Quantum Electron. 2003; 9(6): 1502–1511.

[25] Lita A. E., Miller A. J., and Nam S. W. Counting near-infrared single-photons with 95% efficiency. Opt. Express 2008; 16(5): 3032–3040.

[26] Shibata H., Shimizu K., Takesue H., and Tokura Y. Superconducting nanowire single-photon detector with ultralow dark count rate using cold optical filters. Appl. Phys. Express 2013; 6: 072801.

[27] Chen S., Liu D., Zhang W., You L., He Y., Zhang W., Yang, X. Wu G., Ren M., Zeng H., Wang Z., Xie X., and Jiang M. Time-of-flight laser ranging and imaging at 1550 nm using low-jitter superconducting nanowire single-photon detection system. Appl. Optics 2013; 52(14): 3241–3245.

[28] Li H. W., Kardynal B. E., See P., Shields A. J., Simmonds P, Beere H. E., and Ritchie D. A. Quantum dot resonant tunneling diode for telecommunication wavelength single photon detection. Appl. Phys. Lett. 2007; 91(7): 073516.

[29] Ren M., Wu G., Wu E, and Zeng H. Experimental demonstration of counterfactual quantum key distribution. Laser Phys. 2011; 21(4): 755–760.

[30] Liu Y., Chen T., Wang L, Liang H., Shentu G., Wang J., Cui K., Yin H., Liu N., Li L., Ma X., Pelc J. S., Fejer M. M., Peng C., Zhang Q., and Pan J. Experimental measurement-device-independent quantum key distribution. Phys. Rev. Lett. 2013; 111: 130502.

[31] Takesue H., Nam S. W., Zhang Q., Hadfield R. H., Honjo T., Tamaki K., and Yamamoto Y. Quantum key distribution over a 40-dB channel loss using superconducting single-photon detectors. Nat. Photonics 2007; 1: 343–348.

[32] Ren M., Gu X., Liang Y., Kong W., Wu E, Wu G., and Zeng H. Laser ranging at 1550 nm with 1-GHz sine-wave gated InGaAs/InP APD single-photon detector. Opt. Express 2011; 19(14): 13497–13502.

[33] McCarthy A., Ren X., Frera A. D., Gemmell N. R., Krichel N. J., Scarcella C., Ruggeri A., Tosi A., and Buller G. S. Kilometer-range depth imaging at 1550 nm wavelength using an InGaAs/InP single-photon avalanche diode detector. Opt. Express 2013; 21(19): 22098–22113.

[34] Liang Y., Huang J., Ren M., Feng B., Chen X., Wu E, Wu G., and Zeng H. 1550-nm time-of-flight ranging system employing laser with multiple repetition rates for reducing the range ambiguity. Opt. Express 2014; 22(4): 4662–4670.

[35] Mora A. D., Tosi A., Zappa F., Cova S., Contini D., Pifferi A., Spinelli L., Torricelli A., and Cubeddu R. Fast-gated single-photon avalanche diode for wide dynamic range near infrared spectroscopy. IEEE J. Sel. Top. Quantum Electron. 2010; 16(4): 1023–1030.

[36] Xu L., Wu E, Gu X., Jian Y., Wu G. and Zneg H. High efficiency InGaAs/InP-based single photon detector with high speed. Appl. Phys. Lett. 2009; 94(16): 161106.

[37] Chen X., Wu E, Xu L., Liang Y., Wu G. and Zneg H. Photon-number resolving performance of the InGaAs/InP avalanche photodiode with short gates. Appl. Phys. Lett. 2009; 95(13): 131118.

[38] Namekata N., Adachi S., and Inoue S. 1.5 GHz single-photon detection at telecommunication wavelengths using sinusoidally gated InGaAs/InP avalanche photodiode. Opt. Exp. 2009; 17(8): 6275–6282.

[39] Namekata N., Adachi S., and Inoue S. Ultra-low-noise sinusoidally gated avalanche photodiode for high-speed single-photon detection at telecommunication wavelengths IEEE Photon. Tech. Lett. 2010; 22(8): 529–531.

[40] Yuan Z. L., Kardynal B. E., Sharpe A. W., and Shields A. J. High speed single photon detection in the near infrared. Appl. Phys. Lett. 2007; 91(4): 041114.

[41] Yuan Z. L., Sharpe A. W., Dynes J., Dixon A., and Shields A. J. Multi-gigahertz operation of photon counting InGaAs avalanche photodiodes. Appl. Phys. Lett. 2010; 96: 071102.

[42] Zhang J., Eraerds P., Walenta N., Barreiro C., Thew R., and Zbinden H. 2.23 GHz gating InGaAs/InP single-photon avalanche diode for quantum key distribution. Proc. SPIE, 2010; 7681: 76810Z.

[43] Restellil A., Bienfang J. C., and Migdall A. L. Single-photon detection efficiency up to 50% at 1310 nm with an InGaAs/InP avalanche diode gated at 1.25 GHz. Appl. Phys. Lett. 2013; 102: 141104.

[44] Gu X., Huang K., Pan H., Wu E, and Zeng H. Photon correlation in single-photon frequency upconversion. Opt. Express 2012; 20(3): 2399–2407.

[45] Gu X., Li Y., Pan H., Wu E, and Zeng H. High-speed single-photon frequency upconversion with synchronous pump pulses. IEEE J. Sel. Top. Quantum Electron. 2009; 15: 1748–1752.

[46] Huang K., Gu X., Pan H., Wu E, and Zeng H. Synchronized fiber lasers for efficient coincidence single-photon frequency upconversion. IEEE J. Sel. Top. Quantum Electron. 2012; 18: 562–566.

[47] Liang Y., Wu E, Chen X., Ren M., Jian Y., Wu G., and Zeng H., Room-temperature single-photon detector based on InGaAs/InP avalanche photodiode with multichannel counting ability. IEEE Photon. Tech. Lett. 2011; 23(2): 115–118.

[48] Tomita A., and Nakamura K. Balanced, gated-mode photon detector for quantum-bit discrimination at 1550 nm. Opt. Lett. 2002; 27: 1827–1829.

[49] Comandar L. C., Frohlich, B. Lucamarini M., Patel, K. A. Sharpe A. W., Dynes J. F., Yuan Z. L., Penty R. V., and. Shields A. J. Room temperature single-photon detectors for high bit rate quantum key distribution. Appl. Phys. Lett. 2014; 104: 021101.

[50] Chen X. L., Wu E, Wu G., and Zeng H. P. Low-noise high-speed InGaAs/InP-based single-photon detector. Opt. Exp. 2010; 18(7): 7010–7018.

[51] Wu G., Jian Y., Wu E, Zeng H. Photon-number-resolving detection based on InGaAs/InP avalanche photodiode in the sub-saturated mode. Opt. Exp. 2009; 17(21): 18782–18787.

[52] Jian Y., Wu E, Wu G., and Zeng H. P. Optically self-balanced InGaAs-InP Avalanche photodiode for Infrared single-photon detection. IEEE Photon. Tech. Lett. 2010; 22(3): 173.

[53] Jian Y., Wu E, Chen X., Wu G., and Zeng H. Time-dependent photon number discrimination of InGaAs/InP avalanche photodiode single-photon detector. Appl. Opt. 2011; 50(1): 61–65.

[54] Huang K., Gu X., Ren M., Jian Y., Pan H., Wu G., Wu E and Zeng H. Photon-number-resolving detection at 1.04 μm via coincidence frequency upconversion. Opt. Lett. 2011; 36(9): 1722–1724.

[55] Huang K., Gu X., Pan H., Wu E, and Zeng H. Few-photon-level two-dimensional infrared imaging by coincidence frequency upconversion. Appl. Phys. Lett. 2012; 100(15): 151102.

[56] Zhou Q., Huang K., Pan H., Wu E, and Zeng H. Ultrasensitive mid-infrared up-conversion imaging at few-photon level. Appl. Phys. Lett. 2013; 102(24): 241110.

[57] Chen J., Wu G., Li Y., Wu E and Zeng H. P. Active polarization stabilization of optical fibers suitable for quantum key distribution. Opt. Express 2007; 15(26): 17928–17936.

[58] Chen J., Wu G., Xu L. L., Gu X. R., Wu E, Zeng H. P. Stable quantum key distribution with active polarization control based on time-division multiplexing. New J. Phys. 2009; 11: 065004.